

PAPER • OPEN ACCESS

Development of a 3-y-old Pediatric Cervical Spine Finite Element Model

To cite this article: Na Li *et al* 2019 *IOP Conf. Ser.: Mater. Sci. Eng.* **542** 012035

View the [article online](#) for updates and enhancements.



IOP | ebooks™

Bringing you innovative digital publishing with leading voices to create your essential collection of books in STEM research.

Start exploring the collection - download the first chapter of every title for free.

Development of a 3-y-old Pediatric Cervical Spine Finite Element Model

Na Li¹, Wei Wei², Siwen Wu³, Xian ping Du², Yin Liu¹ and Pengfei Rong^{1,*}

¹ Xiangya 3rd hospital, Central South University, 138th Tongzipo Rd, Changsha 410013, China

² State Key Laboratory of Advanced Design and Manufacturing for Vehicle Body, Hunan University, 1st Lushan South Rd, Changsha 410082, China

³ Xiangya 2nd hospital, Central South University, 139th Renmin Rd, Changsha 410013, China

*Corresponding author: Rongpengfei66@163.com

Abstract

A 3-year-old pediatric cervical spine finite element (FE) model with detailed anatomical and material properties was developed and validated against cadaver tests under both quasi-static loadings. First, bone geometry was reconstructed based on high-resolution computed tomography (CT) scans, and elastic-plastic material was defined to simulate the cortical and cancellous bones. To simulate various ligament tears during dynamic tensile, ligament failure was defined using force versus displacement curves, which had a sigmoidal shape governed by three control points. To better represent the complicated structure of the disc, nucleus pulposus, annulus fibrosus substrate and four pairs of reinforced fiber lamina, intervertebral discs were defined using composite materials combined with viscoelastic material, hill foam material and four pairs of reinforced fiber lamina, respectively. This FE model could be utilized in prediction of cervical spine fracture, ligament and disc tear underlying pediatric cervical injuries.

1. Introduction

As the number of people using modern transportation continues to increase, the number of traffic accidents also increases each year, and it is widely accepted that traffic accidents are a major cause of human fatalities[1]. Recently, considerable attention has been paid to the pediatric cervical spine due to its increased vulnerability to injury. It has been shown that upper spinal injuries caused by sudden deceleration resulting from vehicle crash or direct impact in the case of pedestrians frequently occur in the 0-6 year age group[18]. Three years of age is an important growth period for the pediatric cervical spine. The fusion of the posterior synchondrosis first occurs at this age, and the anterior and posterior ossification centers join at this age as well[2]. These unique anatomical characteristics might cause common pediatric upper cervical injuries in 3-year-old children, including occipitoaxial joint dislocation, atlantoaxial joint dislocation, atlantoaxial rotatory subluxation, and spinal injury without radiological



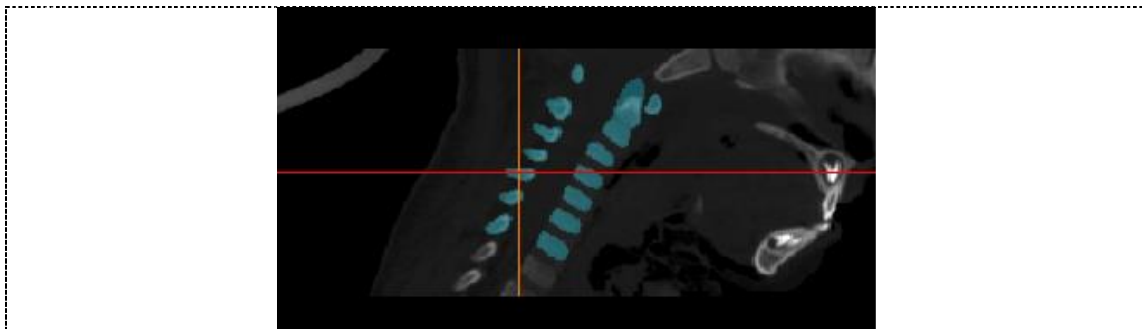
abnormalities[8]. To predict the cervical spine injury in 3-year-old children, it is necessary to develop a higher anatomical and mechanical biofidelity finite element (FE) model.

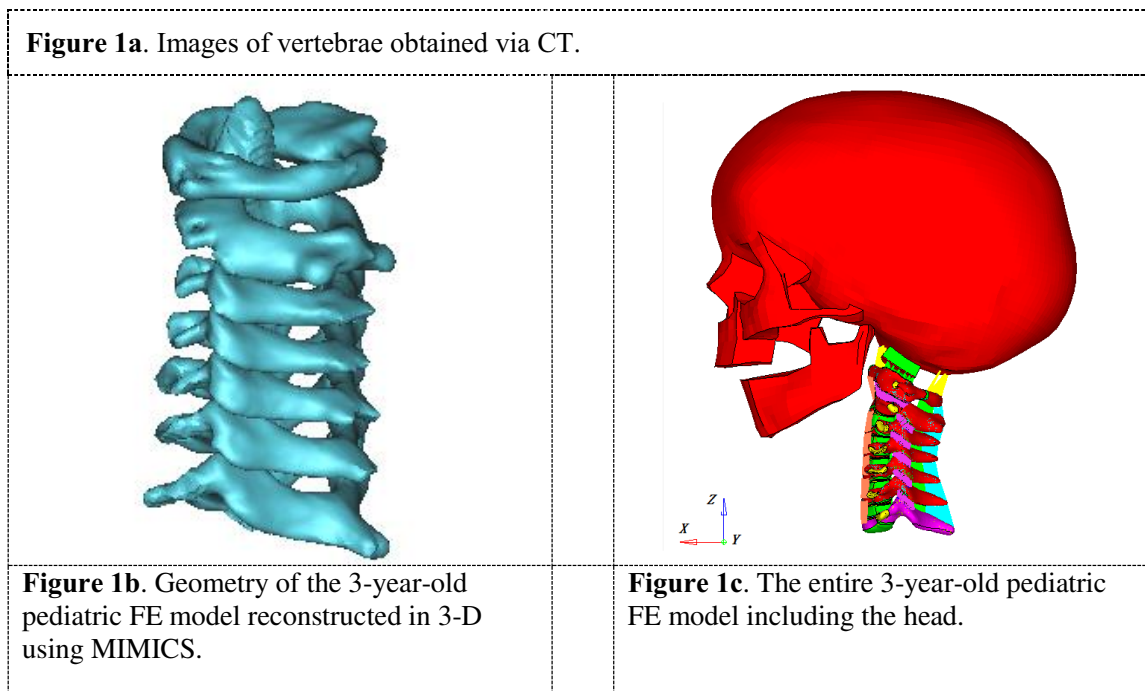
Experimental data obtained from human cadavers available for pediatric cervical spine studies are insufficient in this regard. Over the past three decades, while numerous adult FE models have been developed, only a handful of pediatric FE models have become available[4]. Applying the scaling method proposed by Melvin[15], then a series of pediatric cervical segmental FE models (1 year old, 3 years old, and 6 years old) were developed by scaling an adult cervical spine FE model. Although these models can simulate the pediatric facet joint and nucleus morphology in a satisfactory manner, the material properties of the annulus fibers and other unique morphological features of the pediatric cervical spine were inaccurate because of the limitations of the medical imaging techniques available at that time. Mizuno et al. [16] developed a 3-year-old whole-body human FE model in which both the geometry and material properties were linearly scaled from an adult model (THUMS AM50, Toyota, Japan). The authors validated this model against a 3-year-old dummy test, but it had the same limitations as Kumaransan's FE models[11].

In this study, the objective was to develop a 3-year-old cervical spine FE model with nonlinear material properties. Because it involves all of these methods, our proposed FE model might predict the cervical spine fracture, ligament and disc tear underlying pediatric cervical injury, which would present injury response in traffic accident and the designment of better for 3-year-old children protection system in vehicle.

2. Materials and methods

The images of vertebrae shown in Figure 1a were obtained from a 3-year-old boy (the cause of death was aplastic anemia and infection) with a height (93 cm) and weight (16 kg) similar to average 3-year-old pediatric. The images were obtained using CT scans (Brilliance CT, Philips Medical Systems, Best, The Netherlands) with a 1-mm slice thickness, and the screen resolution of 512×512 pixels. All procedures followed guidelines that were approved by the Central South University Xiangya 3rd Hospital Ethics Committee. Geometric data for the osseous structures were 3-D reconstructed using MIMICS (Version 12, Materialise Inc., Leuven, Belgium), as shown in Figure 1b. The geometries of the ligaments, cartilage, and intervertebral discs not visible in the CT images were filled in between the bony segments based on pediatric cervical anatomy and pediatric spinal models[9]. We adopted a multi-block approach to efficiently meshes. Hypermesh 10.0 (Altair, Troy, MI) was utilized to generate the meshes, as shown in Figure 1c. All calculations were conducted using LS-DYNA version 971 solver (LSTC, Livermore, CA).





The material properties for the 3-year-old cervical spine model are showed in Table 1. According to Gilsanz et al.[7], the scale factor according the adult material properties of the cortical and cancellous bones was 0.805. The material parameters of cortical and cancellous bones for FE modeling of the adult spine reported by Panzer et al[17]. were utilized to derive the cortical and cancellous bones for modeling the 3-year-old pediatric cervical spine.

Table 1. Material properties parameters for the 3-year-old pediatric cervical spine FE model.

Tissue name	Element type	Material model	Material parameter	Scale factor
Cortical bone	Shell	Power-law plasticity	$\rho=1.61 \text{ g/cm}^3$, $E=13.52 \text{ GPa}$, $\mu=0.3$, $K=354.8 \text{ MPa}$, $N=0.2772$	0.805 [7]
Cancellous bone	Hexahedron	Power-law plasticity	$\rho=0.87 \text{ g/cm}^3$, $E=234 \text{ MPa}$, $\mu=0.3$ $K=5.7 \text{ MPa}$, $N=0.2741$	0.805 [7]
Endplate	Shell	Power-law plasticity	$\rho=1.61 \text{ g/cm}^3$, $E=4.48 \text{ GPa}$, $\mu=0.3$, $K=153.2 \text{ MPa}$, $N=0.2772$	0.805 [7]
Annulus ground substance	Hexahedron	Hill Foam	$m=3$, $n=2$, $C1=1.5341 \text{ MPa}$, $b1=1$, $C2=-1.652 \text{ MPa}$, $b2=2$, $C3=0.624 \text{ MPa}$, $b3=3$	0.705 [15]
Annulus fibers	Shell	Fabric	Stress versus strain curve	0.705 [15]

Nucleus	Hexahedron	General viscoelastic	G0=1.72 GPa G1=0.5930 kPa, β1=0.001477 1/s, G2=0.6763 kPa, β2=0.061524 1/s, G3=0.9516 kPa, β3=1.017893 1/s, G4=2.0384 kPa, β4=13.20041 1/s,	1
Growth plate	Hexahedron	Isotropic elastic	ρ=1.36 g/cm ³ , E=25 MPa, μ=0.4	1
Endplate cartilage	Hexahedron	Isotropic elastic	ρ=1.36 g/cm ³ , E=21.25 MPa, μ=0.4	0.85 [15]
Transverse cartilage	Hexahedron	Isotropic elastic	ρ=1.36 g/cm ³ , E=21.25 MPa, μ=0.4	0.85 [15]
Vertebral cartilage	Hexahedron	Isotropic elastic	ρ=1.36 g/cm ³ , E=21.25 MPa, μ=0.4	0.85 [15]
Facet cartilage	Hexahedron	Isotropic elastic	ρ=1.36 g/cm ³ , E=8.13 MPa, μ=0.4	0.782 [15]
Ligaments	Beam spring	Non-linear	Force versus displacement curves	0.744 [15]
Dimensional scale factor G_s				0.637 [27]

E, Young’s modulus; μ, Poisson’s ratio; ρ, density, K, strength coefficient; N, hardening exponent; m, n, C_i, b_i, material constant; G_i, viscoelastic modulus; β_i, viscoelastic exponent.

Based on the 3-year-old cartilage scale factor of 0.85 [7] and the adult cervical spine study reported by Yamada et al. [21], the Young’s modulus values for the pediatric transverse process cartilage, vertebra cartilage and facet joint cartilage were calculated. The disc of the 3-year-old cervix was composed of the annulus fibrosus, the nucleus pulposus, the endplate cartilage and the growth plate to represent the anatomy and material properties of the annulus fibrosus. The substrate of the annulus fibrosus was simulated using *MAT_HILL_FOAM material in LS-DYNA to model non-linear mechanical behavior. Adult annulus fibrosus substrate stress versus stretch curves were measured by Fujita et al. [6] with axial tensile and compression experiments. Yoganandan et al. [26] reported a scale factor for the 3-year-old pediatric cervical spine of 0.705. As shown in Figure 2a, with engineering stress equation (1) as the objective function, we first obtained the material parameters C_j and B_j , which are listed in Table 1. We then referred to a study that used FE modeling of the nucleus by Fice[5] and simulated the nucleus using a viscoelastic material. Combining this with the scale factor reported by Yoganandan et al. [26], we obtained the material parameters shown in Table 1.

$$S_1 = \sum_{j=1}^m C_j (\lambda_1^{b_j-1} - \lambda_1^{\frac{-nb_j}{2n+1}-1}) \tag{1}$$

Here, S_1 represents engineering stress, $m = 3$, and $n = 2$.

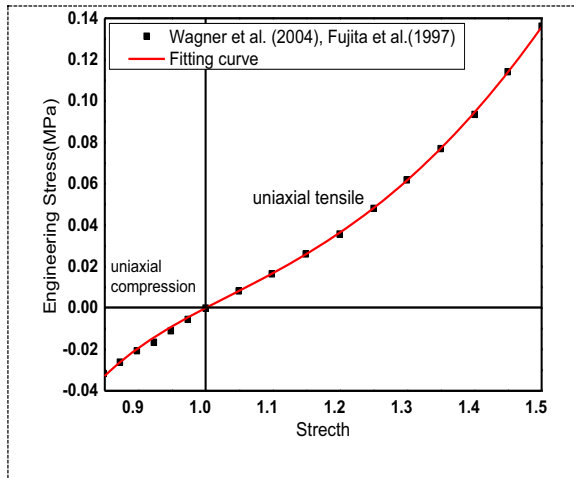


Figure 2a. Stress versus stretch curve of the annulus fibrosus substrate of the 3-year-old pediatric cervical spine, with the stretch being equal to the engineering strain plus one.

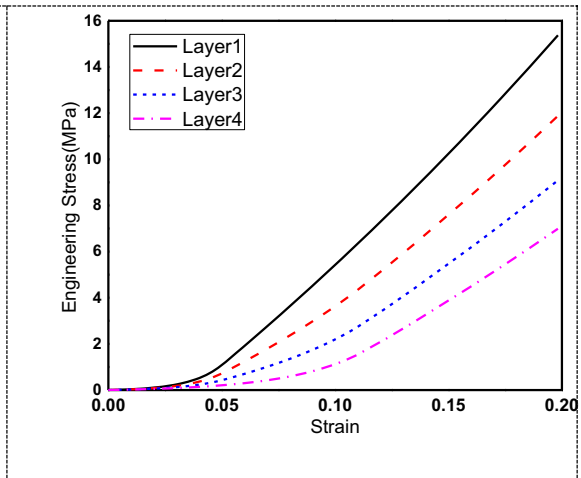


Figure 2b. Engineering stress versus strain curves of the four layers of pediatric AF fiber lamina [19].

The four pairs of reinforced fiber lamina were embedded in the substrate of the annulus fibrosus. The direction of the fibers in each lamina typically vary from $\pm 25^\circ$ in the outer layers to $\pm 45^\circ$ in the inner layers, as measured in the transverse plane of the disc, as shown in the Figure 3a. Using axial tensile experiments on the outer and inner layers of the adult disc AF fiber lamina and the scale factor reported by Yoganandan et al. [26], engineering stress versus strain curves for four layers of pediatric AF fiber lamina were obtained using the linear interpolation method, as shown in Figure 2b.

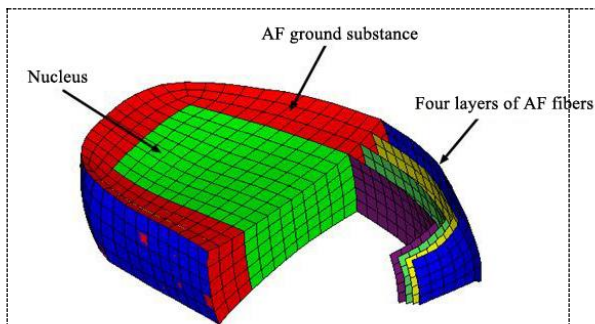


Figure 3a. Disc and fiber orientations of the complex structure simplified into four layers.

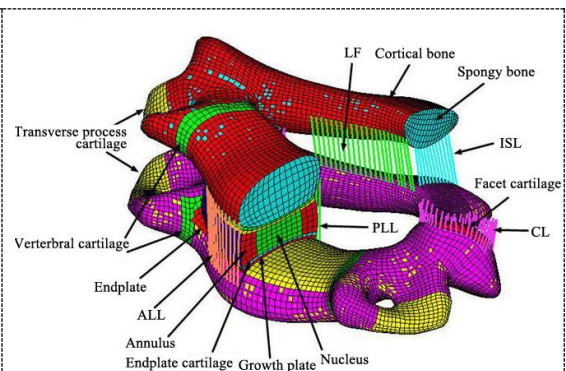


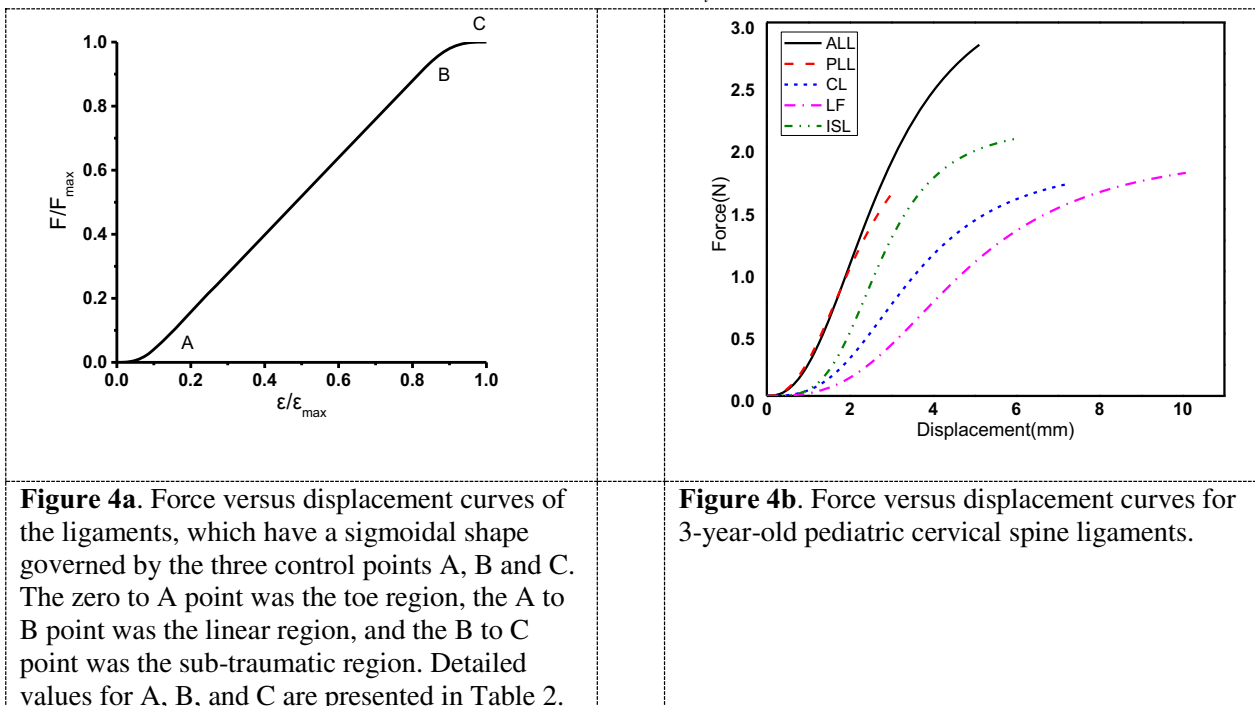
Figure 3b. Sectioned isometric view of the C4-C5 segment model (ALL-anterior longitudinal ligament, PLL-posterior longitudinal ligament, CL-capsular ligament, LF-ligamentum flavum, ISL-interspinous ligament).

Yoganandan et al. [26] reported an adult disc failure force of 571 N. Using the scale factor from equation (2), the disc failure force of a 3-year-old pediatric cervical spine was calculated to be 163 N. In this equation, F_{max} represents the adult disc failure force, the disc material scale factor α is 0.705, and the disc transverse area scale factor α'_A is the squared value of the geometric scale factor (G_s), which is 0.637 [13]. DeWit and Cronin [3] further defined disc failure stress as the ratio of failure force to transverse area. Thus, the failure stress of the endplate and growth plate was 13.8 Mpa.

$$f = F_{max} \times \alpha \times \alpha'_A \tag{2}$$

The ligaments were also simulated by force versus displacement curves, which had a sigmoidal shape governed by three control points, as shown in Figure 4a. The failure strain and force for adult cervical spine ligaments in C2-C7 and C0-C2, which was also utilized in Dong’s 10-year old pediatric cervical spine FE modeling[4], either reported by Yoganandan et al. [26]. In our study, equation (3) was developed by improving upon an equation reported in Dong’s study [4], in which the failure stress and failure strain of 3-year-old pediatric cervical spine ligaments were calculated from the adult data. The force versus displacement curve for 3-year-old pediatric cervical spine ligaments was then obtained using logistic regression curve fitting, as shown in Figure 4b.

$$\left. \begin{aligned} d_i &= \frac{1}{\alpha \times G_s} \times \varepsilon_{max} \left(\frac{\varepsilon_i}{\varepsilon_{max}} \right) \times l_p \\ f_i &= \frac{G_s \times F_{max} \times \left(\frac{F_i}{F_{max}} \right)}{N_i} \end{aligned} \right\} \tag{3}$$



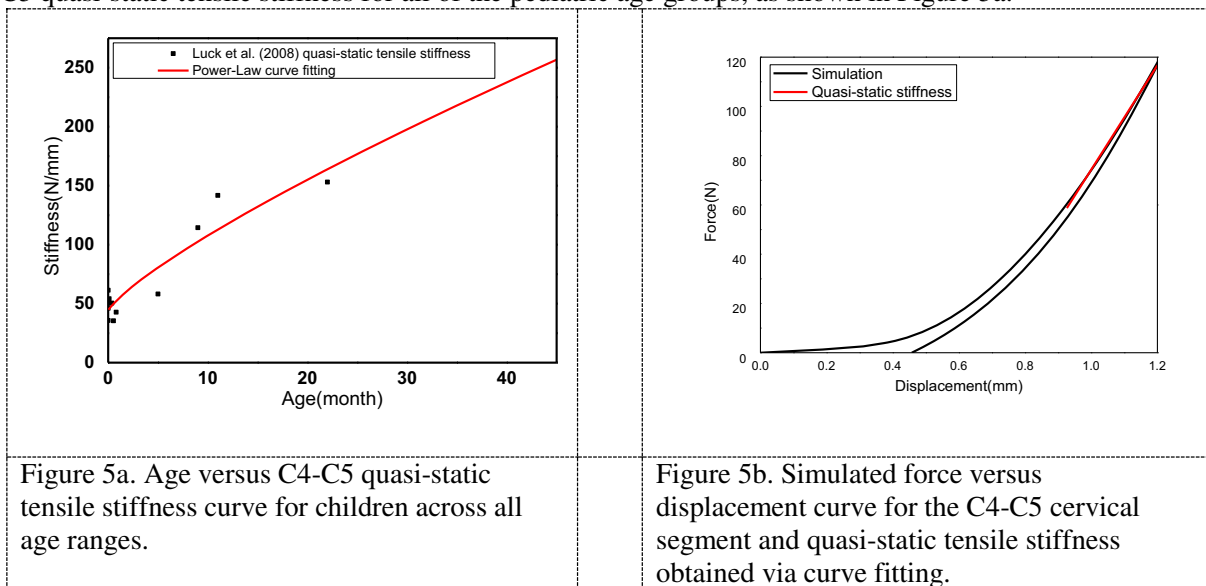
In equation (3), $i = 1, 2, \text{ and } 3$ represent three control points; $\epsilon_3 = \epsilon_{\max}$; $F_3 = F_{\max}$; d_i represents the deflection of the ligament at the three control points; l_P is the length of the ligament; F_i is the force acting on the ligament at the three control points; α is the scale factor for the material properties of the ligaments, which is 0.744; and G_s , the dimensional geometrical scale factor, is 0.637 [26].

Because ligaments are sensitive to strain rate, the visco-elastic material parameters for 3-year-old pediatric cervical spine ligaments had to be included in the FE model. Yoganandan et al. [25] reported ligament tensile responses at different strain rates.

In summary, the 3-year-old cervical spine FE model has 278,492 elements and 243,901 nodes, including 1,384 1-D beam elements, 84,066 2-D shell elements, 192,940 3-D hexahedral elements, and 102 triangular prism elements, in which the element size ranges from 0.5 to 1.0 mm. The head was simulated as a rigid body element.

3. Results

Limited experimental data have been reported for the pediatric cervical spine. Luck et al. [13] utilized cadaver specimens ranging from 20 weeks to 18 years old in quasi-static experiments to obtain axial tensile stiffness, failure force and failure displacement. Because the specimen ages were distributed from neonate to 22 months and 72 months to 216 months, precise data for 36 months were lacking. Therefore, we used the non-linear power-law function equation (4) to represent the relationship between age and C4-C5 quasi-static tensile stiffness for all of the pediatric age groups, as shown in Figure 5a.



$$Y = A \bullet X^B + C \tag{4}$$

Here, Y is the quasi-static tensile stiffness, X is the age (in months), and the undetermined parameters A , B and C were determined by curve fitting. After curve fitting, the correlation coefficients between the curve and the experimental data were $R^2=0.87836$, $A=10.063$, $B=0.802$, and $C=45.34$. Based on this curve, the 3-year-old pediatric quasi-static tensile stiffness was found to be 223.5 N/mm.

In the quasi-static tensile experiment reported by Luck et al. [13], the C4 upper surface was constrained to six degrees of freedom, whereas the loading was applied to the lower surface of C5. The loading rate

was 25.7 N/s, and the load was set to 120 N under quasi-static loading conditions. The force versus displacement curve was compared to the experimental data.

In our quasi-static validation, quasi-static tensile stiffness for C4-C5 segment motion was determined using linear logical regression analysis under loading of 50% to 100%. As shown in Figure 5b, the correlation coefficient between the curve and the experimental data was $R^2=0.998$, and the stiffness was 211.8 N/mm. Compared to the experimental quasi-static tensile stiffness shown in Figure 5a, the deviation was 5.5%.

4. Discussion

The pediatric cervical spine is significantly different from the adult spine with regard to its anatomical and material properties[27]. In this study, the C2-C7 cervical segmental response was first validated under quasi-static loading, then compared with both segmental and global experimental data. However, muscles were not included in this model because accurate muscle force is dependent on physiological cross-section area (PCSA), muscle activation level and muscle fiber length [2], which were unavailable for the 3-year-old pediatric cervical spine [11].

The validation results indicated that the quasi-static stiffness is well correlated with experimental values. Which were within the range of baseline responses or experimental corridors, indicating that all of the segmental FE models have good biofidelity.

In the quasi-static validations, the simulated ROM values were in the range of the experimental corridor, and the deviations relative to the experimental reference value were 14.1%, 7.4% and 1.7%. In contrast, under quasi-static axial rotation loading, the simulated ROM value exceeded the maximum value of the experimental corridor, and the maximum deviation relative to the maximum experimental value was 7.0%. This result indicated that this model could represent 3-year-old C4-C5 cervical extension-flexion and lateral bending responses under 0.905 Nm and 0.517 Nm quasi-static loading.

5. Conclusions

In this study, a 3-year-old cervical spine FE model was developed that includes C0-C7 cervical vertebra, intervertebral discs, cartilage and ligaments. The elastic-plastic material used was defined to simulate the cortical and cancellous bones, and the nucleus pulposus and annulus fibrosus were defined using composite materials combined with viscoelastic material, hill foam material and four pairs of reinforced fiber lamina. The model could be further improved by performing additional experiments involving 3-year-old cervical spine muscles to obtain more accurate material parameters and geometric data.

6. References

- [1] Basu S. 2012. Spinal Injuries in Children. *Med Monatsschr* 3: 441-444.
- [2] Christophy M, Senan NAF, Lotz JC, O' Reilly OM. 2012. A Musculoskeletal Model for the Lumbar Spine. *Biomech. Model. Mechanobiol.* 11: 19-34.
- [3] DeWit JA, Cronin DS. 2012. Cervical Spine Segment Finite Element Model for Traumatic Injury Prediction. *J. Mech. Behav. Biomed.* 10: 138-150.
- [4] Dong L, Li G, Mao H, Marek S, Yang KH. 2013. Development and Validation of a 10-Year-Old Child Ligamentous Cervical Spine Finite Element Model. *Ann. Biomed. Eng.* 41: 2538-2552.
- [5] Fice JB, Cronin DS, Panzer MB. 2011. Cervical Spine Model to Predict Capsular Ligament Response in Rear Impact. *Ann. Biomed. Eng.* 39: 2152-2162.
- [6] Fujita Y, Duncan NA, Lotz JC. 1997. Radial Tensile Properties of the Lumbar Annulus Fibrosus are Site and Degeneration Dependent. *J. Orthop. Res.* 15: 814-819.
- [7] Gilsanz V, Perez FJ, Campbell PP, Dorey FJ, Lee DC, Wren TA. 2009. Quantitative CT Reference Values for Vertebral Trabecular Bone Density in Children and Young Adults 1. *Radiology* 250: 222-227.

- [8] Hamilton MG, Myles ST. 1992. Pediatric spinal injury: review of 174 hospital admissions. *Journal of Neurosurgery* 77: 700-704.
- [9] Holzapfel GA, Schulze-Bauer CAJ, Feigl G, Regitnig P. 2005. Single Lamellar Mechanics of the Human Lumbar Anulus Fibrosus. *Biomech. Model. Mechanobiol.* 3: 125-140.
- [10] Irwin A, Mertz HZ. 1997. Biomechanical Basis for the CRABI and Hybrid III Child Dummies. Pages 261-274. *Child Occupant Protection 2nd Symposium Proceedings*, SAE Technical Paper 973317. Orlando, FL: SAE Conference Proceedings P-316.
- [11] Kumaresan S, Yoganandan N, Pintar FA, Maiman DJ, Kuppa S. 2000. Biomechanical study of pediatric human cervical spine: a finite element approach. *J Biomech Eng* 122: 60-71.
- [12] Lavallee AV5, Ching RP, Nuckley DJ. 2013. Developmental Biomechanics of Neck Musculature. *J. Biomech.* 46: 527-534.
- [13] Luck JF, Nightingale RW, Loyd AM, Prange MT, Dibb AT, Song Y, Fronheiser L, Myers BS. 2008. Tensile Mechanical Properties of the Perinatal And Pediatric PMHS Osteoligamentous Cervical Spine. *Stapp Car Crash J.* 52: 107.
- [14] Mccall T, Fassett D, Brockmeyer D. 2006. Cervical spine trauma in children: a review. *Neurosurgical Focus* 20: E5.
- [15] Melvin JW. 1995. Injury Assessment Reference Values for the Crabi 6-Month Infant Dummy in a Rear-Facing Infant Restraint with Airbag Deployment. SAE Technical Paper. Report no. 0148-7191.
- [16] Mizuno K, Iwata K, Deguchi T, Ikami T, Kubota M. 2005. Development of a Three-Year-Old Child FE Model. *Traffic Inj. Prev.* 6: 361-371.
- [17] Panzer MB, Fice JB, Cronin DS. 2011. Cervical Spine Response in Frontal Crash. *Med. Eng. Phys.* 33: 1147-1159.
- [18] Ruge JR, Sinson GP, McLone DG, Cerullo LJ. 1988. Pediatric Spinal Injury: The Very Young. *J. Neurosurg.* 68: 25-30.
- [19] Wagner DR, Lotz JC. 2004. Theoretical Model and Experimental Results for the Nonlinear Elastic Behavior of Human Annulus Fibrosus. *J. Orthop. Res.* 22: 901-909.
- [20] Xu J, Li Y, Lu G, Zhou W. 2009. Reconstruction model of vehicle impact speed in pedestrian - vehicle accident. *International Journal of Impact Engineering* 36: 783-788.
- [21] Yamada H, Evans FG. 1970. *Strength of Biological Materials*. Baltimore: Williams & Wilkins.
- [22] Yoganandan N, Kumaresan S, Pintar FA. 2000a. Geometric and Mechanical Properties of Human Cervical Spine Ligaments. *J. Biomech. Eng.* 122: 623-629.
- [23] Yoganandan N, Kumaresan S, Pintar FA 2001. Biomechanics of the Cervical Spine Part 2. Cervical Spine Soft Tissue Responses and Biomechanical Modeling. *Clin. Biomech.* 16: 1-27.
- [24] Yoganandan N, Nahum AM, Melvin JW. 2015. *Accidental Injury: Biomechanics and Prevention*. New York, NY: Springer.
- [25] Yoganandan N, Pintar F, Butler J, Reinartz J, Sances AJ, Larson SJ. 1989. Dynamic Response of Human Cervical Spine Ligaments. *Spine* 14: 1102-1110.
- [26] Yoganandan NA, Kumaresan S, Pintar FA. 1998. Pediatric Cervical Spine Biomechanics Using Finite Element Models. Pages 349-363. *Proc. International Research Council on the Biomechanics of Injury Conference: International Research Council on Biomechanics of Injury*.
- [27] Yoganandan NA, Pintar FA, Kumaresan S, Gennarelli TA, Sun E, Kuppa S, Maltese MR, Eppinger RH. 2000b. Pediatric and Small Female Neck Injury Scale Factors and Tolerance Based on Human Spine Biomechanical Characteristics. Pages 345-359. *Proc. International Research Council on the Biomechanics of Injury Conference: International Research Council on Biomechanics of Injury*.